Effect of anions on the memory effect in the tetra-*n*-butylammonium dicarboxylate semiclathrate hydrate reformation

Kazuhiro Minamikawa[a,b], *Jin Shimada*[a,b,c], *Takeshi Sugahara*[a,b,*], *Takayuki Hirai*[a,b]

[a] Division of Chemical Engineering, Department of Materials Engineering Science, Graduate School of Engineering Science, Osaka University, 1-3 Machikaneyama, Toyonaka, Osaka, 560-8531, Japan

[b] Division of Energy and Photochemical Engineering, Research Center for Solar Energy Chemistry, Graduate School of Engineering Science, Osaka University, 1-3 Machikaneyama, Toyonaka, Osaka, 560-8531, Japan

[c] Research Fellow of Japan Society for the Promotion of Science, 5-3-1 Kojimachi, Chiyoda-ku, Tokyo 102-0083, Japan.

*Corresponding author E-mail: sugahara.takeshi.es@osaka-u.ac.jp

KEYWORDS. Semiclathrate hydrate, thermal storage material, memory effect, crystallization, supercooling

ABSTRACT

Semiclathrate hydrates (SCHs) have been expected to be one of the phase change materials for cold energy storage. The large degree of supercooling in SCH formation, however, is a major obstacle to practical applications of SCHs. As a way to suppress the degree of supercooling, we focused on the memory effect (a kind of temperature hysteresis) in the tetra-*n*-butylammonium dicarboxylate SCHs. The tartarate, malate, and succinate anions, which have similar chemical structures, were used as anions. As a result, the ability to retain the memory effect in the TBA-tartarate SCH was the largest of the three SCHs. The interaction of the substituted hydroxy group(s) of anions with surrounding water molecules in the aqueous solution might improve the thermal stability of the solution structure that causes the memory effect, resulting in promoting the SCH reformation.

1. INTRODUCTION

Unused thermal energy has been released from various energy-consuming points, such as vehicles, life, and factories, to environment. Phase change materials (PCMs) have abilities not only to store unused thermal energy but also to contribute to filling the gap between electric power generation and demand. Ice is known as one of the famous PCMs, whereas the melting temperature of ice is too low for storage of vegetables, fruits[1], and vaccines[2,3]. One of the promising PCMs is semiclathrate hydrate (SCH). SCH is a crystalline compound consisting of host water molecules and appropriate guest substances[4–9]. The typical guest substances of SCHs are tetra-*n*-butylammonium (TBA) and tetra-*n*-butylphosphonium (TBP) salts. The cations are

enclathrated in polyhedral cages and the anions form hydrogen-bonded networks with the host water molecules[4-9]. The nitrogen atom in the TBA cation and the phosphorus atom in the TBP cation are placed in the center of the four cages. Unlike gas hydrates that commonly form at high pressures, SCH can crystallize just by cooling the TBA (or TBP) salt aqueous solution at atmospheric pressure. Tetra-*n*-butylammonium bromide (TBA-Br) SCH with the hydration number of 26 has the dissociation temperature of 285.57 K and the relatively large dissociation enthalpy (192±3 $kJ \cdot kg^{-1}$) at 0.1 MPa[10]. Taking advantage of such characteristics, TBA-Br SCH slurry has been utilized at shopping malls and offices in Japan as air-conditioning media[11].

Thermodynamic properties of SCHs strongly depend on the combination of cations and anions[4,5,12]. Thermodynamic properties of SCHs are suitable for PCMs in cold chains because of not only the equilibrium temperatures within 270 to 300 K at atmospheric pressure but also the relatively large enthalpy of dissociation (160-220 $kJ \cdot kg^{-1}$)[10-22]. According as the working temperatures of PCMs required in cold chains, the development of SCHs with various equilibrium temperatures is essential. For example, SCHs with various equilibrium temperatures are suitable for cooling of lithium-ion batteries (288 to 308 K)[23], other than for the storage of vegetables and fruits (280 to 283 K)[1] and vaccines (275 to 281 K)[2,3] and for air conditioning (278 to 288 K)[11,21].

SCH crystallization often requires a degree of supercooling as large as that of ice, which prevents its practical use as a PCM. Supercooling is a phenomenon in which an aqueous solution does not crystallize even when cooled below its crystallization temperature. An efficient supercooling suppression surely reduces the energy and cost of SCH formation. Therefore, many studies have been conducted to suppress the supercooling of ice or SCH formation. Inada et al.[24] reported that an ultrasonic approach strongly promotes ice formation. Okawa et al.[25] studied the

elimination of supercooling by applying an electric field to supercooled water. Researches on suppressing the supercooling have been also conducted in TBA-Br aqueous solution. Kumano et al.[26] applied an electric field using various metal electrodes to suppress the supercooling of TBA-Br SCH. Machida et al.[27,28] and Oshima et al.[29] reported on the hysteresis phenomenon (called the memory effect), which is one of the methods to suppress supercooling. The memory effect is a phenomenon in which crystallization occurs at a small degree of supercooling or short induction time when crystals are formed from the resultant aqueous solution after the SCH dissociation. Oshima et al.[29] reported that the recrystallization of TBA-Br SCH occurs at almost the same place as the previous crystal dissociation. They also reported that the recrystallization probability decreased with physical stimuli, such as stirring the solution just after the end of dissociation. Machida et al.[27] reported that the memory effect remained for a short period at temperatures up to 287.2 K, which is approximately 2 K higher than the equilibrium temperature of TBA-Br SCH ($T_{eq.}$= 285.57 K). They also observed the scanning electron microscopic images of the solution structures (20 nm in diameter) remaining in the aqueous solution after complete TBA-Br SCH dissociation[27,28]. The existence of residual solution structures in the aqueous solution causes the memory effect.[27,28] The memory effect has been also reported in gas hydrates, where the memory effect could be caused by the existence of anomalous dissolved gas[30], solution structure[31-35], or ultra-fine bubbles (so-called nanobubbles)[36].

Here, we focused on the residual solution structures because semiclathrate hydrates were treated without any gas species. In the case of TBA-halide SCHs like TBA-Br SCH, some of the water molecules in the cage structure are replaced with halide anions. In the case of TBA-lactate SCH, the oxygen atoms in the carboxy and hydroxy groups of the lactate anion substitute the water molecules[37]. This means that the interaction of hydroxycarboxylate (HDC) anions with the

surrounding water molecules is different from that of halide anions. Therefore, in the present study, we investigated the memory effect of SCH reformation for SCHs with carboxy and hydroxy groups in the anions: L-malate (-Mala) and L-tartarate (-Tar), which have structures with one and two hydroxy group(s) to the structure of succinate (-Suc), respectively (Fig. 1). It has been reported that the maximum equilibrium temperatures of TBA-Tar, TBA-Mala, and TBA-Suc SCHs are 279.54 K[38,39], 284.2 K[38], and 286.1 K[5,38], respectively. When the aqueous solution was prepared at the stoichiometric composition of SCH, the SCH was completely dissociated at the maximum equilibrium temperature.

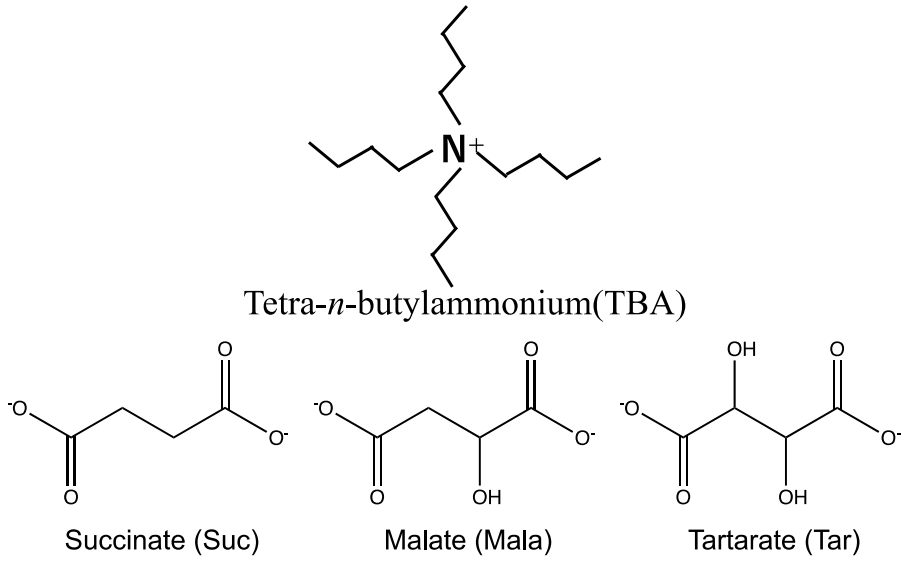

Figure 1. Chemical structures of TBA cation and dicarboxylate anions used in the present study.

2. EXPERIMENTAL

2.1. Materials

TBA-based salts were synthesized by neutralization reaction of tetra-*n*-butylammonium hydroxide with the corresponding acids in the aqueous solution. Neutralization reactions were performed for 24 hours. The products were confirmed by ^{1}H and ^{13}C nuclear magnetic resonance (NMR, JEOL, ECS-400). There were no impurity-derived signals or anomalies in the integral ratio. The purity of the synthesized TBA-based salts was equal to or higher than that originally contained in the synthesis reagents.

2.2. Apparatus and procedures

Approximately 15 cm^3 of aqueous solutions were prepared at the stoichiometric compositions x = 0.0162 (w = 0.366) for TBA-Tar[39], x = 0.0156 (w = 0.352) for TBA-Mala[38], and x = 0.0159 (w = 0.360) for TBA-Suc[5,38] with the electric balance (Shimadzu, AUW220D) with an uncertainly of 0.2 mg. The symbols x and w represent the mole and mass fractions of salts in the aqueous solution, respectively.

Schematic illustration of the experimental setup was shown in Figure 2. Each aqueous solution was dispensed into the fifteen screw vials by approximately 1 cm^3, which were put into a propylene glycol bath thermostated with a cooling medium circulator (Taitec, CL-80R). Firstly, the system temperature was kept at 291 K for enough duration and then decreased to 263 K at a cooling rate of 0.1 K/min with the program unit (Taitec, PU-5). The system temperature was raised at a heating rate of 0.2 K/min until the temperature reached to a target temperature (T_{target}) beyond the equilibrium temperature of an SCH. After the temperature was held for 30 min at

each target temperature, the cooling process to 263 K was started at a cooling rate of 0.1 K/min. The same processes were repeated while the target temperature was increased by a step of 1 K (Figure 3). To detect the crystallization temperature ($T_{cry.}$) in each SCH system, a T-type thermocouple was inserted to every screw vial. The thermocouples were connected to the data logger (Toho, TRM-00J). The crystallization temperature was defined as the onset temperature when the temperature of the aqueous solution rose rapidly by the enthalpy of SCH formation.

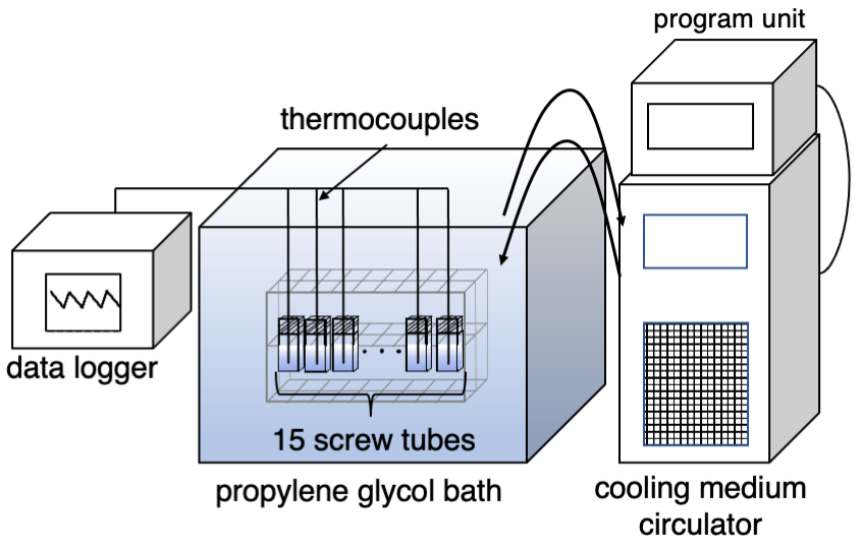

Figure 2. Schematic illustration of the experimental setup. 15 screw vials were placed in a propylene glycol bath thermostated with a cooling medium circulator.

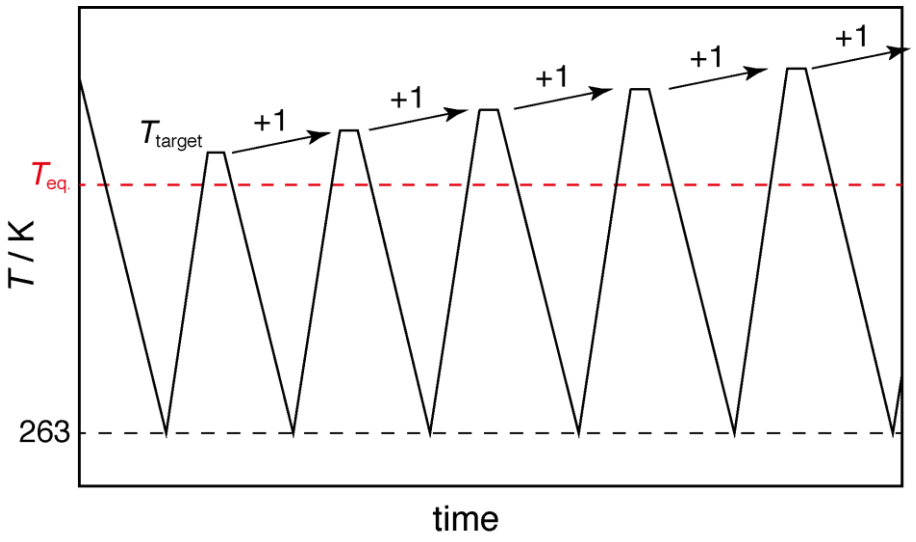

Figure 3. Schematic illustration of programmed temperature profile for the investigation of the memory effect. The cooling and heating rates were 0.1 K/min and 0.2 K/min, respectively. The holding duration at each target temperature (T_{target}) was 30 min.

We also used a micro differential scanning calorimeter (DSC) (Setaram, μDSC VIIevo). Approximately 20 mg of the prepared TBA-HDC aqueous solutions were loaded into the DSC cell. The precise sample mass of the loaded aqueous solutions was measured with the electric balance (A&D, BM-22) with an uncertainty of 0.02 mg. The uncertainty of the temperature in the DSC measurements based on the melting temperatures of water and naphthalene was 0.06 K. The program of the DSC furnace temperature was almost the same as that in the direct measurements with screw vials. In the DSC measurements, the effect of the holding duration at each target temperature was investigated.

3. RESULTS AND DISCUSSION

The degree of supercooling ($\Delta T_{sup.}$) was defined as the difference ($T_{eq.}$–$T_{cry.}$) between the equilibrium temperature ($T_{eq.}$) and the crystallization temperature ($T_{cry.}$). The crystallization temperature $T_{cry.}$ of TBA-Tar SCH was 268.2±1.0 K in the aqueous solution without the memory effect as well as fresh aqueous solution experiencing no SCH crystallization, where the average $\Delta T_{sup.}$ was 11.3 K because the $T_{eq.}$ of TBA-Tar SCH was 279.54 K. With the memory effect, TBA-Tar SCH recrystallized at $T_{cry.}$ = 274.2±1.5 K which is 6.0 K higher than the $T_{cry.}$ without the memory effect.

To investigate the temperature durability of the memory effect, the $T_{cry.}$ of TBA-Tar SCH was measured with changing the target temperature (T_{target}) from 285.2 K to 296.2 K by a step of 1.0 K, as shown in Figure 3. The temperature was held for 30 min at each T_{target}. Note that the period where the temperatures were beyond $T_{eq.}$ = 279.54 K (heating period from $T_{eq.}$ to T_{target} and cooling from T_{target} to $T_{eq.}$) might be a significant factor to bear in mind. The effect of the temperature-holding duration at a T_{target} will be discussed later. The obtained $\Delta T_{sup.}$ are shown in Figure 4a. $\Delta T_{sup.}$ in the cases of T_{target} from 285.2 K to 290.2 K were suppressed within 5.3 K, whereas $\Delta T_{sup.}$ were approximately 11.3 K in the cases of T_{target} over 292.2 K where the memory effect disappeared. The T_{target} between 290.2 K and 291.2 K was the border where the memory effect can be retained for 30 min in the TBA-Tar aqueous solution.

In addition to the TBA-Tar SCH, the temperature durability of the memory effect for TBA-Mala ($T_{eq.}$=284.2 K) and TBA-Suc ($T_{eq.}$=286.1 K) SCHs was also investigated. The obtained $\Delta T_{sup.}$ are shown in Figures 4b and 4c. The crystallization temperatures ($T_{cry.}$) of TBA-Mala and TBA-Suc SCHs in the aqueous solution without the memory effect were 269.5±1.0 K and 270.0±1.0 K, where the average $\Delta T_{sup.}$ were 14.7 K and 16.1 K, respectively. With the

memory effect, the average $\Delta T_{sup.}$ of TBA-Mala and TBA-Suc SCHs were suppressed to 5.9 K and 6.5 K respectively, though $\Delta T_{sup.}$ for TBA-Mala SCH has a dispersion slightly larger than that of TBA-Tar and TBA-Suc SCHs. The border (T_{border}) of the target temperatures where the memory effect can be retained for 30 min were between 291.2 K and 292.2 K for TBA-Mala SCH and between 292.2 K and 293.2 K for TBA-Suc SCH.

The equilibrium temperature ($T_{eq.}$) and the border (T_{border}) of the target temperature for TBA-Tar, TBA-Mala, and TBA-Suc SCHs are summarized in Table 1. TBA-Suc SCH with the highest $T_{eq.}$ had the highest T_{border} of three SCHs. This is reasonable because the solution structure, remaining in the aqueous solution after complete SCH dissociation above $T_{eq.}$, causes the memory effect[27–29]. To compare the effects of the anions, we considered the difference between T_{border} and $T_{eq.}$ as listed in Table 1. Considering the temperature durability of the memory effect through the difference between T_{border} and $T_{eq.}$, the temperature range where the memory effect can be retained in the TBA-Tar SCH system was the widest of the three SCH systems investigated in the present study. The temperature ranges where the memory effect was retained in the TBA-Mala and TBA-Suc SCH systems were narrower than that of the TBA-Tar SCH system, but much wider than that of the TBA-Br SCH system[27].

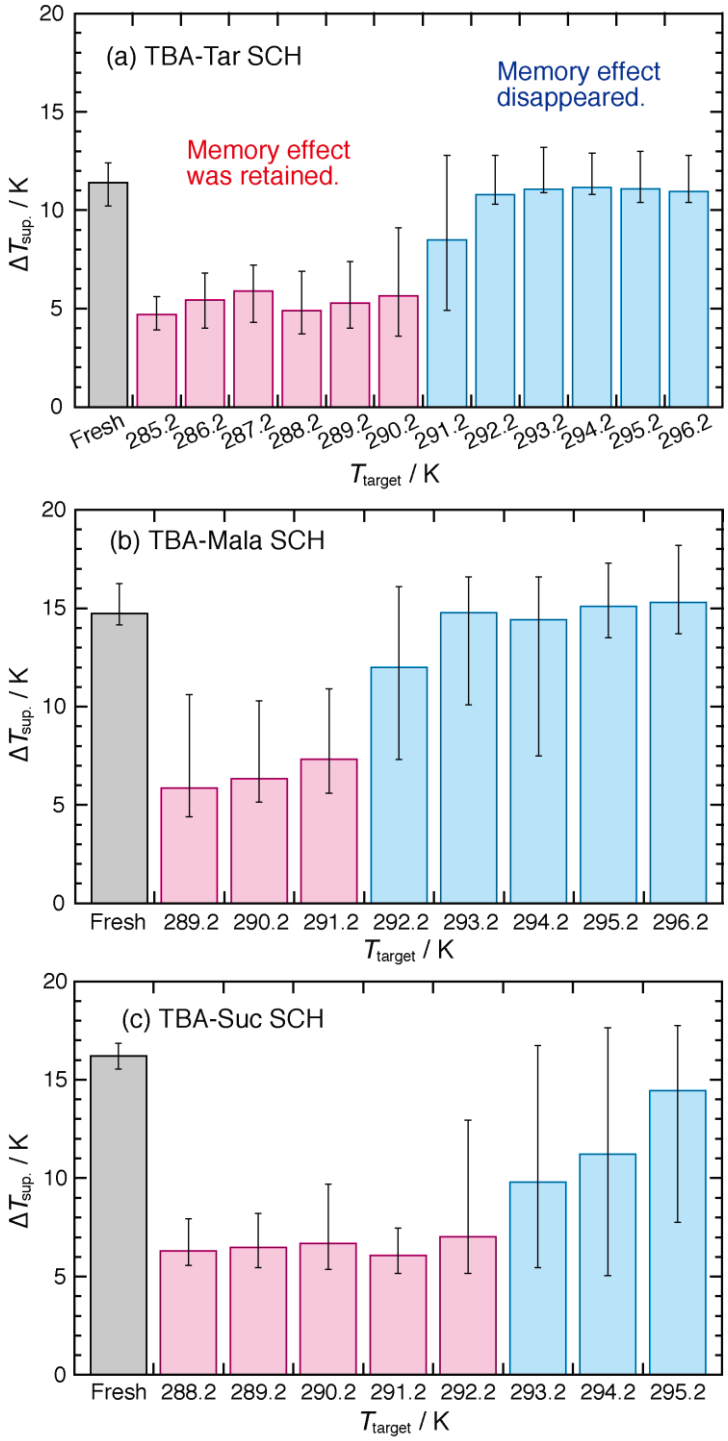

Figure 4. Effect of target temperatures (T_{target}) on the degree of supercooling ($\Delta T_{sup.}$) in the SCH formation of (a) TBA-Tar, (b) TBA-Mala, and (c) TBA-Suc. The temperature was held for 30 min at each T_{target}.

Table 1. Equilibrium temperature ($T_{eq.}$), the border (T_{border}) of the target temperature where the memory effect can be retained for 30 min, and these difference (T_{border}–$T_{eq.}$) in the TBA-Tar, TBA-Mala, and TBA-Suc SCHs.

SCH	$T_{eq.}$ / K	T_{border} / K	(T_{border}- $T_{eq.}$) / K
TBA-Tar	279.5	290.7±0.5	11.2±0.5
TBA-Mala	284.2	291.7±0.5	7.5±0.5
TBA-Suc	286.1	292.7±0.5	6.6±0.5

The duration for which the memory effect can be retained is significant and interesting. The memory effect of TBA-Br SCH ($T_{eq.}$ = 285.57 K) can be retained for at least 30 min at 286.2 K and only for approximately 20 sec at 287.2 K[27]. We focused on the effect of the temperature-holding duration at three T_{target} of 288.2 K, 289.2 K and 290.2 K in the TBA-Tar SCH system ($T_{eq.}$ = 279.5 K). The results are shown in Figure 5. The memory effect persisted even after held at 288.2 K and 289.2 K for 8 hours and 5 hours, respectively. At 290.2 K, by contrast, it was retained for 30 min, whereas it disappeared after held for 1 hour. These results reveal that the lifetime of the memory effect gets shorter as the target temperature approaches the border temperature.

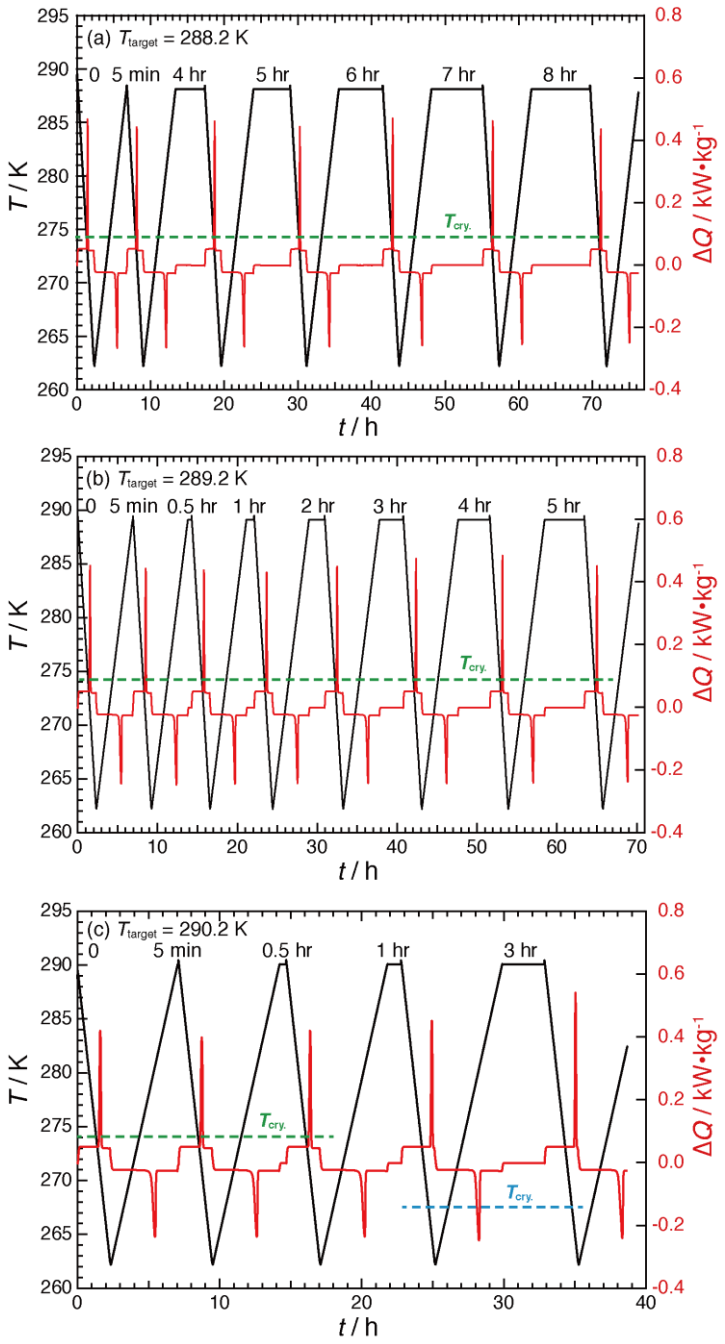

Figure 5. DSC results of the memory effect of TBA-Tar SCH reformation at T_{target} of 288.2 K, 289.2 K, and 290.2 K. The results at 288.2 K and 289.2 K were independent of the temperature holding duration measured in the present study, whereas the memory effect disappeared after the temperature holding at 290.2 K for 1 hour.

Why did the TBA-Tar SCH system have such a temperature-resistant memory effect stronger than TBA-Br SCH? We believe that this results from the hydrogen-bonded interaction of the Tar anion with the water molecules. It has been reported that the hydration numbers of the TBA-Tar, TBA-Mala, and TBA-Suc SCHs are 60.8[39], 63[38], and 62.6[5,38], respectively. The hydration number of the TBA-Tar SCH is approximately 2.0 smaller than those of TBA-Mala and TBA-Suc SCHs despite having the same crystal structure. This means that the two hydroxy groups, as well as the two carboxy groups included in the Tar anion, take part in the cage structure instead of two water molecules, whereas the hydroxy group of TBA-Mala SCH would not replace water molecule in the cage structure because TBA-Mala and TBA-Suc SCHs have almost the same hydration number. In addition, in the TBA-Br SCH, Br anion also takes part in the cage structure instead of a water molecule. According to recent quasi-elastic neutron scattering studies[40], water reorientation around the Br anion is quite fast. Such fast water reorientation causes relatively early breakage of the residual solution structures.

4. CONCLUSION

The memory effect in the reformation of the SCHs with environmentally-friendly anions was investigated. In the present study, we focused on the memory effect of SCHs including three kinds of hydroxycarboxylate anions: Tar (2OH groups + Suc); Mala (OH group + Suc); Suc. These SCHs had a relatively strong memory effect, rather than TBA-Br SCH previously reported[27]. The type of anion affected how long and how high temperature the memory effect of SCH reformation can be retained.

The temperature durability of the memory effect was evaluated through the difference between the border temperature and the equilibrium temperature. As shown in Table 1, the

temperature difference of the TBA-Tar SCH was the largest of the three SCHs. Those of TBA-Mala and TBA-Suc SCHs were comparable. More hydrogen-bonded interactions of the Tar anion with the water molecules would result in such a highly temperature-resistant memory effect in TBA-Tar SCH reformation.

In the TBA-Tar SCH system where the most temperature-resistant memory effect was exhibited, we investigated the duration for which the memory effect could be retained. As the target temperature approached the border temperature, the lifetime of the memory effect in the aqueous solution got shorter. At a temperature 10 K higher than the equilibrium temperature, nevertheless, the memory effect persisted for more than 5 hours in the TBA-Tar SCH system.

From the viewpoint of the memory effect, SCHs with environmentally-friendly hydroxycarboxylate (-Tar and -Mala) anions, instead of halide anions, have the potential to be promising phase change materials.

AUTHOR INFORMATION

Corresponding Author

*(T.S.) Tel and Fax: +81-6-6850-6293. E-mail: sugahara.takeshi.es@osaka-u.ac.jp.

ORCID

Jin Shimada: 0000-0002-9720-5963

Takeshi Sugahara: 0000-0002-5236-5605

Takayuki Hirai: 0000-0003-4747-4919

Funding Sources

This work was supported by JSPS KAKENHI Grant-in-Aid for JSPS Fellows (JP21J20788 and JP22KJ2069 for J.S.) and Grant-in-Aid for Scientific Research (JP22K05050 for T.S.).

Notes

The authors declare no competing financial interest.

ACKNOWLEDGMENT

The authors acknowledge scientific support from the Gas-Hydrate Analyzing System (GHAS) of the Division of Chemical Engineering, Department of Materials Engineering Science, Graduate School of Engineering Science, Osaka University.

REFERENCES

(1) Xu, X.; Zhang, X. Simulation and experimental investigation of a multi-temperature insulation box with phase change materials for cold storage, *J. Food Eng.* **2021***, 292*, 110286. DOI: 10.1016/j.jfoodeng.2020.110286

(2) Davis, H.; Dow, T.; Isopi, L.; Blue, J. T. Examination of the effect of agitation on the potency of the Ebola Zaire vaccine rVSVΔG-ZEBOV-GP, *Vaccine* **2020**, *38*, 2643−2645. DOI: 10.1016/j.vaccine.2020.02.002

(3) American Hospital Association, Special Bulletin, COVID-19 vaccine storage requirement, 2021. https://www.aha.org/system/files/media/file/2021/03/aha-releases-covid-19-vaccine-storage-requirements-infographic-bulletin-3-26-21.pdf (accessed July 3, 2024).

(4) Fowler, D. L.; Loebenstein, W. V.; Pall, D. B.; Kraus, C. A. Some unusual hydrates of quaternary ammonium salts. *J. Am. Chem. Soc.* **1940**, *62*, 1140 − 1142. DOI: 10.1021/ja01862a039

(5) Dyadin, Y.A.; Udachin, K.A. Clathrate polyhydrates of peralkylonium salts and their analogs. *J. Struct. Chem*. **1987**, *28*, 394−432. DOI: 10.1007/BF00753818

(6) Jeffrey, G. A.; Atwood, J. L.; Davies, J. E.; MacNicol, D. D.; Vogtle, F., Eds. *Hydrate Inclusion Compounds*. In Comprehensive Supramolecular Chemistry. Solid State Supramolecular Chemistry: Crystal Engineering. **1996**, 6, 757–788.

(7) Shimada, W.; Shiro, M.; Kondo, H.; Takeya, S.; Oyama, H.; Ebinuma, T.; Narita, H. Tetra-*n*-butylammonium bromide-water (1/ 38). *Acta Crystallogr., Sect. C: Cryst. Struct. Commun*. **2005**, *C61*, o65−o66. DOI: 10.1107/S0108270104032743

(8) Rodionova, T.; Komarov, V.; Villevald, G.; Aladko, L.; Karpova, T.; Manakov, A. Calorimetric and Structural Studies of Tetrabutylammonium Chloride Ionic Clathrate Hydrates. *J. Phys. Chem*. *B* **2010**, *114*, 11838–11846. DOI: 10.1021/jp103939q

(9) Muromachi, S.; Takeya, S.; Yamamoto, Y.; Ohmura, R. Characterization of tetra-*n*-butylphosphonium bromide semiclathrate hydrate by crystal structure analysis. *CrystEngComm* **2014**, *16*, 2056−2060. DOI: 10.1039/C3CE41942H

(10) Sugahara, T.; Machida, H. Dissociation and nucleation of tetra-*n*-butyl ammonium bromide semi-clathrate hydrates at high pressure. *J. Chem. Eng. Data* **2017***,* **62**, 2721−2725. DOI: 10.1021/acs.jced.7b00115

(11) Ogoshi, H.; Takao, S. Air-Conditioning System Using Clathrate Hydrate Slurry. *JFE Technical Report* **2004**, *3*, 1−5.

(12) Nakayama, H.; Watanabe, K. Hydrates of Organic Compounds. II. The Effect of Alkyl Groups on the Formation of Quaternary Ammonium Fluoride Hydrates. *Bull. Chem. Soc. Jpn* **1976**, *49*, 1254−1256. DOI: 10.1246/bcsj.49.1254

(13) Sakamoto, H.; Sato, K.; Shiraiwa, K.; Takeya, S.; Nakajima, M.; Ohmura, R. Synthesis, characterization and thermal-property measurements of ionic semi-clathrate hydrates formed with tetrabutylphosphonium chloride and tetrabutylammonium acrylate. *RSC Adv.*, **2011**, *1*, 315−322. DOI: 10.1039/C1RA00108F

(14) Oshima, M.; Kida, M.; Jin, Y.; Nagao, J. Dissociation behaviour of (tetra-*n*-butylammonium bromide + tetra-*n*-butylammonium chloride) mixed semiclathrate hydrate systems. *J. Chem. Thermodyn.* **2015**, *90*, 277−281. DOI: 10.1016/j.jct.2015.07.009

(15) Muromachi, S.; Takeya, S. Design of thermophysical properties of semiclathrate hydrates formed by tetra-*n*-butylammonium hydroxybutyrate. *Ind. Eng. Chem. Res.* **2018**, *57*, 3059−3064. DOI: 10.1021/acs.iecr.7b05028

(16) Shimada, J.; Shimada, M.; Sugahara, T.; Tsunashima, K.; Tani, A.; Tsuchida, Y.; Matsumiya, M. Phase Equilibrium Relations of Semiclathrate Hydrates Based on Tetra-*n*-

butylphosphonium Formate, Acetate, and Lactate, *J. Chem. Eng. Data* **2018**, *63*, 3615−3620. DOI: 10.1021/acs.jced.8b00481

(17) Arai, Y.; Koyama, R.; Endo, F.; Hotta, A.; Ohmura, R. Thermophysical property measurements on tetrabutylphosphonium sulfate ionic semiclathrate hydrate consisting of the bivalent anion. *J. Chem. Thermodyn*. **2019**, *131*, 330−335. DOI: 10.1016/j.jct.2018.11.017

(18) Koyama, R.; Hotta, A.; Ohmura, R. Equilibrium temperature and dissociation heat of tetrabutylphosphonium acrylate (TBPAc) ionic semi-clathrate hydrate as a medium for the hydrate-based thermal energy storage system. *J. Chem. Thermodyn*. **2020**, *144*, 106088. DOI: 10.1016/j.jct.2020.106088

(19) Shimada, J.; Shimada, M.; Sugahara, T.; Tsunashima, K.; Takaoka, Y.; Tani, A. Phase equilibrium temperature and dissociation enthalpy in the tri-*n*-butylalkylphosphonium bromide semiclathrate hydrate systems. *Chem. Eng. Sci*. **2021**, *236*, 116514. DOI: 10.1016/j.ces.2021.116514

(20) Shimada, J.; Yamada, M.; Tani, A.; Sugahara, T.; Tsunashima, K.; Tsuchida, Y.; Hirai, T. Thermodynamic Properties of Tetra-*n*-butylphosphonium Dicarboxylate Semiclathrate Hydrates, *J. Chem. Eng. Data* **2022**, *67*, 67−73. DOI: 10.1021/acs.jced.1c00741

(21) Yamamoto, K.; Iwai, T.; Hiraga, K.; Miyamoto, T.; Hotta, A.; Ohmura R. Synthesis and thermophysical properties of Tetrabutylammonium picolinate hydrate as an energy storage phase change materials for cold chain. *J. Energy Storage* **2022**, *55*, 105812. DOI: 10.1016/j.est.2022.105812

(22) Azuma, S.; Shimada, J.; Tsunashima, K.; Sugahara, T.; Hirai, T. Effect of introducing a cyclobutylmethyl group into an onion cation on the thermodynamic properties of ionic clathrate hydrate, *New J. Chem*. **2023**, *47*, 231−237. DOI: 10.1039/D2NJ04361K

(23) Chen, D.; Jiang, J.; Kim, G.-H.; Yang, C.; Pesaran, A. Comparison of different cooling methods for lithium ion battery cells, *Appl. Therm. Eng.* **2016**, *94*, 846 − 854. DOI: 10.1016/j.applthermaleng.2015.10.015

(24) Inada, T.; Zhang, X.; Yabe, A.; Kozawa, Y. Active control of phase change from supercooled water to ice by ultrasonic vibration 1. Control of freezing temperature, *Int. J. Heat Mass Transfer* **2001**, *44*, 4523–4531. DOI: 10.1016/S0017-9310(01)00057-6

(25) Okawa, S.; Saito, A.; Harada, T. Experimental Study on the Effect of the Electric Field on the Freezing of the Supercooled Water, *Trans. Japan Soc. Refrigerating Air Conditioning Engineers* **1997**,*14*, 47–55. DOI: 10.11322/tjsrae.14.47

(26) Kumano, H.; Hirata, T.; Mitsuishi, K.; Ueno, K. Experimental study on effect of electric field on hydrate nucleation in supercooled tetra-*n*-butyl ammonium bromide aqueous solution, *Int. J. Refrigeration* **2012**, *35*, 1266–1274. DOI: 10.1016/j.ijrefrig.2012.03.005

(27) Machida, H.; Sugahara, T.; Hirasawa, I. Memory effect in tetra-*n*-butyl ammonium bromide semiclathrate hydrate reformation: the existence of solution structures after hydrate decomposition, *CrystEngComm* **2018**. *20*, 3328–3334. DOI: 10.1039/C8CE00190A

(28) Machida, H.; Sugahara, T.; Masunaga, H.; Hirasawa, I. Calorimetric and Small-Angle X-ray Scattering Studies on the Memory Effect in the Tetra-*n*-butylammonium Bromide Semiclathrate Hydrate System, *J. Cryst. Growth* **2020**, *533*, 125476. DOI: 10.1016/j.jcrysgro.2019.125476

(29) Oshima, M.; Shimada, W.; Hashimoto, S.; Tani, A.; Ohgaki, K. Memory effect on semi-clathrate hydrate formation: A case study of tetragonal tetra-*n*-butyl ammonium bromide hydrate, *Chem. Eng. Sci.* **2010**, *65*, 5442–5446. DOI: 10.1016/j.ces.2010.07.019

(30) Song, K. Y.; Feneyrou, G.; Fleyfel, F.; Martin, R.; Lievois, J.; Kobayashi, R. Solubility measurements of methane and ethane in water at and near hydrate conditions, *Fluid Phase Equilib*. **1997**, *128*, 249–260. DOI: 10.1016/S0378-3812(96)03165-2

(31) Lederhos, J. P.; Long, J. P.; Sum, A.; Christiansen, R. L.; Sloan, E. D., Jr. Effective kinetic inhibitors for natural gas hydrates, *Chem. Eng. Sci.* **1996**, *51*, 1221–1229. DOI: 10.1016/0009-2509(95)00370-3

(32) Takeya, S.; Hori, A.; Hondoh, T.; Uchida, T. Freezing-Memory Effect of Water on Nucleation of CO_2 Hydrate Crystals, *J. Phys. Chem. B* **2000**, *104*, 4164–4168. DOI: 10.1021/jp993759+

(33) Ohmura, R.; Ogawa, M.; Yasuoka, K.; Mori, Y. H. Statistical Study of Clathrate-Hydrate Nucleation in a Water/Hydrochlorofluorocarbon System: Search for the Nature of the "Memory Effect", *J. Phys. Chem. B* **2003**, *107*, 5289–5293. DOI: 10.1021/jp027094e

(34) Sefidroodi, H.; Abrahamsen, E.; Kelland, M. A. Investigation into the strength and source of the memory effect for cyclopentane hydrate, *Chem. Eng. Sci.* **2013**, *87*, 133–140. DOI: 10.1016/j.ces.2012.10.018

(35) Ripmeester, J. A.; Alavi, S. Some current challenges in clathrate hydrate science: Nucleation, decomposition and the memory effect, *Curr. Opin. Solid State Mater. Sci.* **2016**, *20*, 344–351. DOI: 10.1016/j.cossms.2016.03.005

(36) Uchida, T.; Yamazaki, K.; Gohara, K. Gas Nano-Bubbles as Nucleation Acceleration in the Gas-Hydrate Memory Effect, *J. Phys. Chem. C* **2016**, *120*, 26620–26629. DOI: 10.1021/acs.jpcc.6b07995

(37) Muromachi, S.; Abe, T.; Yamamoto, Y.; Takeya, S. Hydration structures of lactic acid: characterization of the ionic clathrate hydrate formed with a biological organic acid anion. *Phys. Chem. Chem. Phys.*, **2014**, *16*, 21467−21472. DOI: 10.1039/C4CP03444A

(38) Nakayama, H.; Watanabe, K. Hydrates of Organic Compounds. III. The formation of Clathrate-like Hydrates of Tetrabutylammonium Dicarboxylates. *Bull. Chem. Soc. Jpn* **1978**, *51*, 2518−2522. DOI: 10.1246/bcsj.51.2518

(39) Minamikawa, K.; Shimada, J.; Sugahara, T.; Hirai, T. Thermodynamic Properties of Tetra-*n*-butylammonium and Tetra-*n*-butylphosphonium Hydroxycarboxylate Semiclathrate Hydrates, *J. Chem. Eng. Data* **2023**, *68*, 3492−3498. DOI: 10.1021/acs.jced.3c00575

(40) Shimada, J.; Tani, A.; Yamada, T.; Sugahara, T.; Hirai, T.; Okuchi, T. Quasi-elastic neutron scattering studies on fast dynamics of water molecules in tetra-*n*-butylammonium bromide semiclathrate hydrate, *Appl. Phys. Lett.* **2023**, *123*, 044104. DOI: 10.1063/5.0157560

TOC